Improving X-ray Laminography from Sparse Data via Spectral Interpolation (SIM)

Ali Benouar A¹, Mohammed Reda Ahmed Bacha¹, Kamel Ghanem Ghalem¹

¹Complex System Laboratory, Higher School of Electrical and Energetic Engineering, Oran, Algeria

Abstract – Laminography is a non-destructive imaging technique widely employed in the industrial sector for the inspection of components using X-ray radiation. It offers several advantages, including high depth resolution, particularly for flat or layered structures. However, the image reconstruction process in laminographic systems—based on stationary inverse-geometry X-ray acquisition—often leads to the appearance of artifacts in the final images, primarily due to the limited number of available projections. In this work, we introduce a spectral interpolation method (SIM) designed to address this limitation by effectively reducing star-shaped artifacts. The performance of the proposed method was evaluated using the Structural Similarity Index (SSIM). Compared to conventional reconstruction approaches, the SIM technique demonstrated significantly improved image quality, particularly in scenarios involving sparse projection datasets

Received: 25/05/2025, Revised: 12/08/2025, Accepted: 30/09/2025

Keywords: X-ray tomography, laminography, CND inspection methodes

I. Introduction

In the industrial sector, non-destructive testing (NDT) plays a crucial role in ensuring manufacturing reliability and maintaining product quality. Among the various NDT techniques, X-ray inspection stands out for its widespread use, owing to its strong penetration capabilities, high sensitivity, and ease of interpretation—making it ideal for revealing internal features of industrial components [1]. X-ray inspection can be implemented through three-dimensional computed tomography (CT), which utilizes X-ray densitometry to generate two-dimensional projection images with a high signal-to-noise ratio (SNR). While CT enables detailed 3D cross-sectional visualization and precise measurements, it is computationally

intensive, as it requires the processing of hundreds of projection datasets [2]. Additionally, CT is less well suited for flat, laterally extended samples—such as circuit boards or biological slides—commonly encountered in the electronics and life sciences industries.

The article opens with a review of the various scan geometries utilized in X-ray laminography, followed by a detailed description of the zero-padding interpolation technique. It then presents the outcomes of simulations and tests performed on digital phantoms, and concludes with the analysis of raw experimental acquisition data.

X-ray laminography acquisition systems typically consist of a mobile X-ray source and a flat-panel detector, enabling the generation of coronal cross-sectional images from a limited

number of projections over a restricted scan area [3]. The imaging approach is conceptually similar to that of digital tomosynthesis (DT), commonly used in medical imaging [4]. One of the key advantages of X-ray laminography lies in its ability to reduce structural superposition, which enhances image clarity in complex objects [5]. Additionally, in comparison to conventional computed tomography (CT), laminography is computationally more efficient due to the reduced number of projections required for image reconstruction. However, the mechanical movement of the source and detector can introduce motion artifacts and increase system complexity, posing challenges to image quality and hardware design [6].

A common scenario in imaging involves flat samples, where one dimension is significantly smaller than the other two. In X-ray (micro)imaging, such samples typically include microelectronic components, artworks, or biological specimens that require nondestructive examination—for example, for in situ observations or to preserve delicate, irreplaceable materials. Figure 1 illustrates two potential scan geometries for these types of samples under parallel beam conditions. In conventional computed tomography (CT), the object is rotated about an axis perpendicular to the X-ray beam direction. This configuration often leads to substantial variations in transmitted intensity across different angles, and in some orientations, transmission may be nearly absent.

The alternative configuration, known as computed laminography (CL), is specifically tailored for imaging flat samples. In CL, the rotation axis is inclined relative to the incoming beam, aligning roughly parallel to the sample surface normal. This setup results in more consistent transmission across all projections, allowing for complete data acquisition. Computed laminography has recently gained traction in industrial non-destructive testing (NDT), as well as in X-ray micro- and nanoimaging and neutron imaging applications [7].

In this work, we propose a spectral interpolation method (SIM) aimed at addressing the limitations of conventional projection-based X-ray tomography. The method incorporates data correction directly into the reconstruction workflow to suppress truncation artifacts and enhance the quantitative accuracy of the resulting images. The effectiveness of the proposed SIM approach is assessed through comparison with established reconstruction techniques.

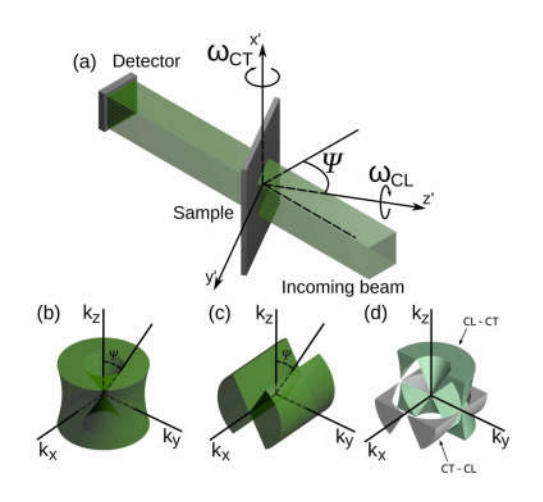


Fig. 1. (a) Illustration of the two scanning geometries for the parallel-beam case. Here ωCT is the tomographic rotation axis and ωCL is the laminographic rotation axis. The specimen coordinate frame (x,y,z) is defined with (x,y) spanning the in-plane direction and z being parallel to the specimen surface normal. (b,c) Sketch of the filling of Fourier space in CL and CT, respectively, for $\Psi=30^\circ$. (d) Sketch of the difference in the filling of the Fourier space for the two methods, with parts cut away for better visualization

II. Theorem of spectral interpolation method (SIM) by zero-padding

Zero-padding (ZP) interpolation approach, involves extending the discrete Fourier transform (DFT) of a finite sequence with zeroes and taking an inverse DFT to generate a more densely sampled version of the original sequence with values interpolated at intermediate positions between the original measured samples [08]. Specifically, one begins by taking the DFT of the sequence g(xn) given by eq01, considered as periodic function that

has period X and which is bandlimited to frequency K. Given $N \ge 2K + 1$ samples of g(x) taken at points $xn = n X / N \ (n = 0, ..., N - 1)$ which is:

$$c_k = \frac{1}{N} \sum_{n=0}^{N-1} g\left(x_n\right) \exp\left(\frac{-j2\pi nK}{N}\right) \tag{1}$$

For $k=0,\ldots,N-1$, where $j=\sqrt{-1}$. Zeropadding involves the creation of a new sequence dk', having $L=n_d$. N, elements (where n_d is an integer). If g(x) is assumed to be band limited to frequency K and if $N \ge 2K+1$, the sequence dk' defined as follows:

$$d_{k'} = \begin{cases} c_{k'} & k' = 0, ..., K \\ 0 & k' = K+1, ..., L-K-1 \\ c_{k'} - L + N & k' = L-K, ..., L-1 \end{cases}$$
 (2)

A more densely sampled sequence $\hat{g}(xi)$, where $\exists i \ X \ / \ L \ (i = 0, ..., L - 1)$, is now obtained by taking the inverse DFT of the sequence dk'.

$$\hat{g}(x_i) = \sum_{n=0}^{N-1} g(x_n) \sigma_N(x_i - x_n)$$
 (3)

For $i=0,\ldots,L-1$. ZP interpolation is generally viewed as a somewhat crude interpolation approach, but this reputation is undeserved.

The main idea of this method is to insert a set of zero value lines symmetrically on the angular dimension of the spectrum resulting from bedimensional Fast Fourrier Transform FFT2D of the set of projection [9]. In the following, we expose the main steps of the algorithm used.

- Let $\{Q_{\theta i}, i = 1, N\}$ be a set of N subsampled projections on 0-360° profile, defined by a $\Delta\theta$ pitch, $\Delta\theta = 1$ °.
- Now let $\{QF_{\theta i}, i = 1,2,3,..., N\}$ be a set of the corresponding FFT2D of $Q_{\theta i}$, defined as:

$$QF_{\theta i} = FFT2D(Q_{\theta i})$$

(4)

 Let QFZ be the zero padding of the set QF, whose elements are defined as follows:

$$QFZ_{\theta i} = \begin{cases} QF_{\theta i} & i = 0, 1, 2, ..., N - 1. \\ 0 & i = -nd \times \frac{N}{2}, ..., -2, -1. \\ 0 & i = N + 1, N + 2, ..., nd \times \frac{N}{2} \end{cases}$$
(5)

- nd, chosen greater than 1,(use Equation 02) is an integer number which defines a multiplying coefficient of the extension rate of QFZ size in the angular dimension, and represents as well the multiplication factor of the initial resolution sinogram Q).
- QZ is defined as the bi-dimensional inverse Fourier transform of QFZ after filtering by a 'ramp-filter' as:

$$QF_{\theta i} = FFT2D(Q_{\theta i})$$

(6)

- Let QFZ be the zero padding of the set QF, whose elements are defined as follows:
- QZ is defined as the bi-dimensional inverse Fourier transform of QFZ after filtering by a 'ramp-filter' as:

$$QZ_{\theta i} = FFT2D^{-1}(QFZ_{\theta i} \times |w|)$$

$$w : being a ramp filter$$
(7)

2.1. Simulation study

In this study, we conducted simulations of our imaging system using MATLAB (version 4.0), modeling an array of X-ray sources and a

x

compact detector. The simulated X-ray source array included multiple focal points to emulate a fan-beam geometry within the object space. The number of projections was chosen to replicate the conditions of the experimental dataset, ensuring consistency in the reconstruction process and the behavior of the proposed SIM method.

The reconstruction was carried out using a filtered back-projection (FBP) algorithm, which offers a well-defined analytical formulation and is theoretically robust. Although interpolation during the projection data transformation can introduce errors [10], numerical simulations provide access to ground-truth values, enabling validation of the conversion algorithm. Additionally, simulations allow precise control over all parameters, isolating the influence of the algorithm on the final result.

Projection data were generated using the TIGRE toolbox—a high-performance simulation framework for cone-beam CT based on MATLAB and CUDA, developed by the University of Bath in collaboration with CERN's CT Laboratory. TIGRE integrates both advanced projection modeling and widely used reconstruction algorithms [11].

2.2. Simulation result

The simulation is performed on Shepp-Logan phantom with a size of 256 *256* 5 mm3, and the Gaussian noise with a variance of 10-6 was added to the phantom for simulating statistical noise. the simulation process consists of generation of projections dataset with 360 projections $\Delta\theta$ =1°, figure 02.



Fig.2.: left: Shepp-Logan phantom phantom right Original Projection
Dataset

The generated dataset is sub simpled to simulated dataset for an acquisition system with poor resolution with 36 projections as shown in figure 3 than we generate interpolated projection by the SIM to create virtual projections that contribute to redusing the noise artifact in the reconstructed image.

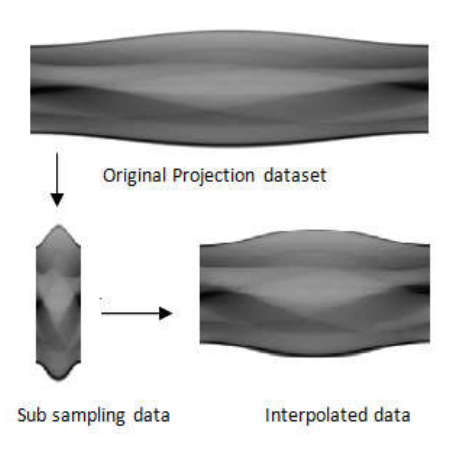


Fig.3. Process of subsampaling projection dataset ans reinterpolated it

Using the simulated projections of the Shepp-Logan phantom, reconstruction was performed via the filtered back-projection (FBP) algorithm [12]. The resulting images from both the subsampled dataset and the SIMinterpolated dataset are presented in Figures 4(B) and 4(C), respectively. The enhanced performance of the SIM interpolation can be attributed to the effective doubling of projection which increases the density backprojection lines while reducing their average intensity [13]-[14]. This is due to the oscillatory nature of the SIM-generated data, which balances the accumulation of positive and negative values at each pixel during reconstruction. As the number of projections increases, the spatial frequency and amplitude of streak artifacts are progressively reduced [15]–[16], thereby diminishing their visual impact. In contrast, direct reconstruction from a sparsely sampled dataset tends to amplify these streak patterns, as it accumulates unbalanced pixel intensities—a phenomenon clearly observable in Figure 4(B) compared to the SIM-corrected result in Figure 4(C) [17].

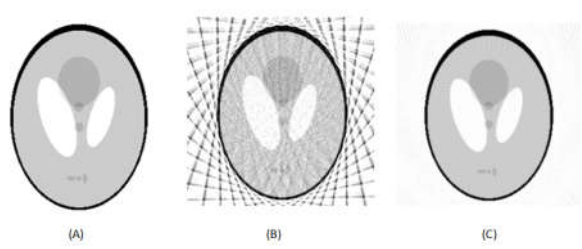


Fig.4. A: The reference images, (B) conventional reconstruction from 36 sub sampling data projections, C. reconstructed image corrected by the SIM interpolation

To quantitatively assess the similarity between the interpolated projections and the ideal reference projections, the Structural Similarity Index (SSIM) [18]–[19] was chosen as the evaluation metric. SSIM provides a measure of perceptual similarity between two images, with values ranging from 0 to 1 — a value of 1 indicating perfect similarity. The mathematical formulation of the SSIM is given as follows:

$$SSIM(x,y) = \frac{(2\mu_x \mu_y + C_1)(2\sigma_{xy} + C_2)}{(\mu_x^2 + \mu_y^2 + C_1)(\sigma_x^2 + \sigma_y^2 + C_2)}$$
(8)

In this equation, x and y denote the two images being compared. The terms μ_x and μ_y represent their respective mean intensities, while σ_x and σ_y correspond to their standard deviations. The covariance between x and y is given by σ_{xy} . Constants C_1 and C_2 are included to prevent division by zero and to stabilize the SSIM computation [20].

Simulations were carried out across various inclination angles α . For each configuration, the SSIM index was computed between the SIM-corrected projection (Figure 5.C) and the ideal projection (Figure 5.A). As illustrated in Figure 6, the accuracy of the projection data

conversion improves progressively as α approaches 0°. Despite the interpolation process introducing some degree of error, the SSIM remains consistently above 0.733 for rotation angles ranging from -28° to $+28^{\circ}$, indicating that the SIM-corrected projections closely approximate a full 360° real-world acquisition around $\alpha = 0^{\circ}$.

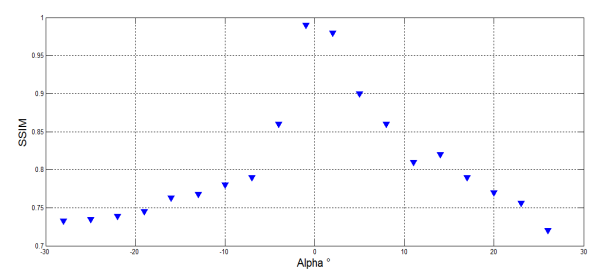


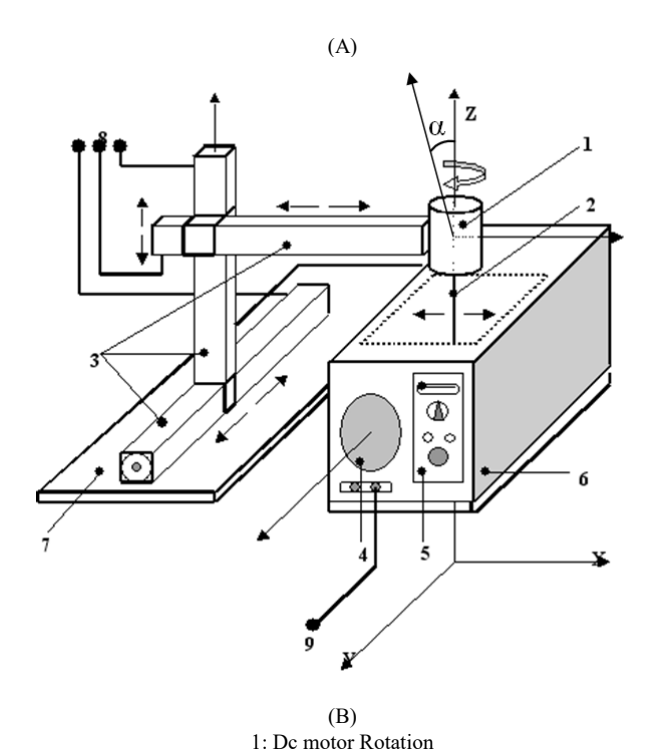
Fig.5. SSIMs between converted projection and ideal projection varies with angles

III. Experimentation and material

Figure 6 shows the sketch map of the experimental system acquisition X-ray projections. The specimen is placed on a stage which has three degrees of freedom. An X-ray source is fixed and deployed on beam profile. The planar detectors is obtained by translation movement of the object by translation robot which is above the stage and can be rotate about an axis. The rotation axis passed in the fan plan of the X-ray and is perpendicular to it. We can move the inclination of the axis of rotation with respect to the X-ray plan by α° (-28° to +28°) for the lamingraphy acquisition protocol. In the process of scanning, the stage and the object and the detector are moved synchronously to keep the cone-beam focusing on the same region. As shown in Fig.6, the whole system is located in a shielding room for radiation protection.

When the object moves along the detector, the source-detector distance is fixed. The stage can move along X, Y and Z directions separately. The magnification of the specimen

can be adjusted by changing the height of the stage. When we finished the acquisition for one projection, the angle α will incremented for the next acquisition. Table 01 shows some parameters of the configuration system. In a specific scanning, the scanning protocol should be optimized.



4: Radiographic screen 5: Panel control 6: X-ray chamber 7: Platforome robot

2: Objet support

3: 3D axis translation robot

Fig.6: Experimental device

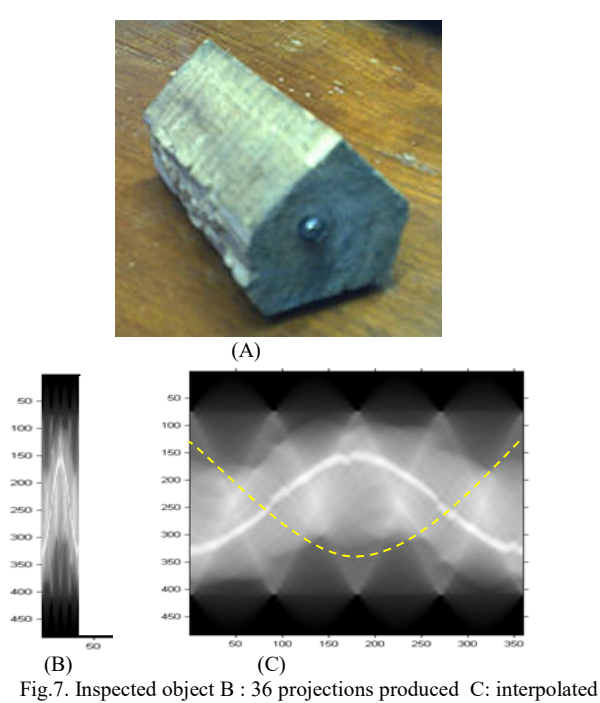
TABLE I SPECIFICATIONS OF EXPERIMENTATION SYSTEM

| X-ray source | 35.25 Kv , 0.6 mA. |
|----------------------|--------------------|
| Detector calibration | 1000 imp/s/V |
| X-ray Filtrage | 2μm alum |
| Resolution | 1mm2 |
| Deflection angle | 20° |

IV. **Experimentation result**

The acquisition system was configured to initially capture 36 projections, forming the original projection dataset. Subsequently, the SIM interpolation method was applied to

enhance angular resolution by generating and injecting 324 additional projections into the dataset. These interpolated projections were computed based on the original set. The test specimen was a pentagon-shaped wooden object measuring $5 \times 4.5 \times 7$ cm, containing a central metal axis, as shown in Figure 7(A). The original and SIM-interpolated projection datasets are illustrated in Figures 7(B) and 7(C), respectively.



data projections 324 projections injected

The same reconstruction process used in the simulation is applied in the same way on the row 36 projections data and the 360 generated projection by SIM. the 36 real projections are conserved and insered in the line retroprojection as we can see in the Figure 8.

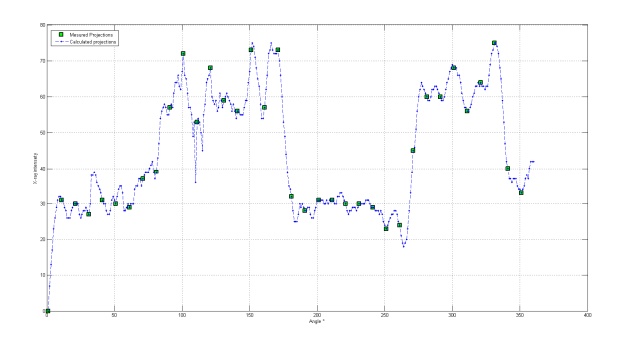


Fig.8: SIM interpolation on a tomographic line for retroprojection in Figure 7 (C).

The result of each reconstruction is showen in figure 09. As illustrating point for our investigations we imaged

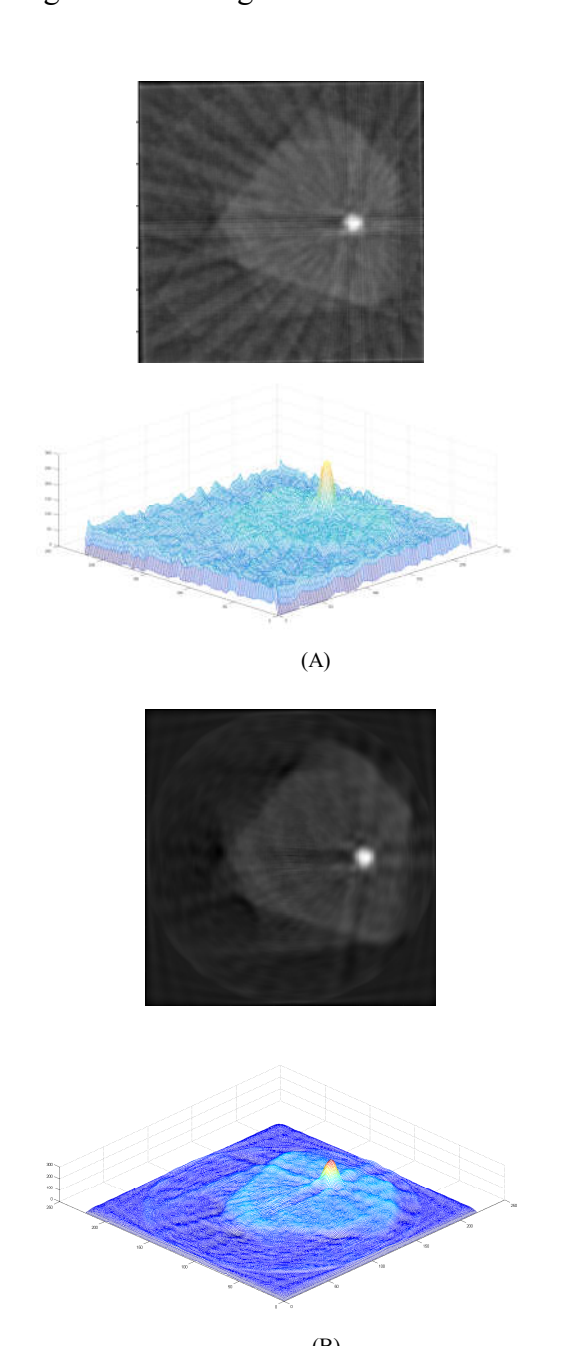


Fig.9, A: Lamingraphy construction from 36 Projections
Construction from 360 projections generated by SIM

The inspected object was imaged using a limited number of projections, resulting in a degraded reconstruction, as illustrated in Figure 9(A). The reconstructed image exhibits

noticeably reduced contrast and is affected by prominent noise in the form of cross-shaped streaks, commonly referred to as the "star effect." This artifact arises from the reconstruction process itself and is particularly pronounced in areas with sharp transitions between materials of differing densities—such as the wood/metal interface in this case—due to the insufficient number of projections.

contrast, Figure 9(B) demonstrates substantial reduction of this artifact, particularly along the radial direction. This improvement highlights a key advantage of tomographic reconstruction: as the number of projections increases, the spatial frequency of the star artifacts rises while their amplitude diminishes. The SIM method enables a significant expansion of projection data—far beyond the of physical limitations the acquisition hardware—by generating synthetic projections with a much higher angular resolution. These virtual projections are then integrated into the reconstruction process, effectively boosting image quality.

To quantitatively evaluate this enhancement, the SSIM metric was employed, as done in the simulation study. For this experimental validation. the acquisition system configured to produce 360 real projections at deflection angles $\alpha = 0^{\circ}$, 10° , and 20° , providing high-fidelity reference images for SSIM computation. The corresponding results are presented in Table II, confirming that SIMenhanced reconstructions maintain a high level of structural similarity even under varying angular conditions.

TABLE II SSIM IN TERMS OF THE ANGLE OF DEFLECTION

| α | SSIM |
|-----|-------|
| 0° | 0.931 |
| 10° | 0.778 |
| 20° | 0.764 |

As anticipated from the simulation results, the SIM method produced reconstructed images that closely matched the reference image when the projection plane was perfectly perpendicular to the X-ray beam. Under these standard tomographic acquisition conditions, interregional contrast was clearly preserved. Furthermore, despite the inherent limitations of the acquisition setup, the SIM method effectively reduced star-shaped noise artifacts and maintained a Structural Similarity Index (SSIM) consistently above 0.764.

V. Results and discussion

In this study, the SIM methods is applied for simulations and experiments, and the quality of corrected images were evaluated by analyzing visual inspection and SSIM.

Fig.8 and table II shows the SSIM betwin reference and reconstructed images for Shepp-Logan phantom and inspected object of the figure 7(A) with diffrents angle of deflection α . The SSIM remained within a decent margin of error and remained above 0.7.

It is important to highlight that the filtered back-projection (FBP) algorithm used in laminographic image reconstruction performs a polar-to-Cartesian estimation of the twodimensional Fourier spectral space. In this context, the SIM method is particularly well suited to complement the FBP algorithm [21], as it also operates within the spectral domain. SIM helps to mitigate the non-uniform distribution of spectral information, particularly in the high-frequency regions that are most susceptible to degradation and are primarily responsible for the emergence of star-shaped artifacts. As a fully digital approach, the SIM technique offers a powerful and efficient way to enhance the angular resolution of the imaging system purely through software, thereby extending the capabilities of the acquisition hardware without physical modification.

VI. Conclusion

In this study, we proposed the SIM method, based on spectral-domain interpolation, as an effective solution to reduce star artifacts that degrade the quality of reconstructed laminographic images. This numerical approach enables a substantial increase in angular density without the need for projection additional physical acquisitions. It highlights the potential of spectral processing to compensate for and even surpass the hardware limitations of low angular resolution imaging systems. The power of spectral interpolation provides a significant precision gain, virtually enhancing the resolution of the acquisition device through purely software-based means.

Looking ahead, this method paves the way for broader applications in imaging shallow-depth structures, particularly on opaque, non-transparent surfaces. It could thus emerge as an economical and competitive alternative to more complex and costly techniques such as Optical Coherence Tomography OCT, (optical coherence tomography), especially in the fields of non-destructive testing, composite material analysis, and surface biomedical imaging.

References

- [1] S.M. Anouncia, R. Saravanan, Non-destructive testing using radiographic images a survey, Insight, *Non-Destructive Testing and Condition Monitoring*, 48 (2006) 592-597.
- [2] Burnyoung Kim, Dobin Yim, Seungwan Lee, Development of a truncation artifact reduction method in stationary inversegeometry X-ray laminography for non-destructive testing, *Nuclear Engineering and Technology* 53 (2021) 1662-1633.
- [3] M. Jatteau, C. Berche, Review of image reconstruction techniques in medical transaxial computed tomography, *Ann. Radiol. 26 (1983)* 13-22.
- [4] F. Xu, L. Helfen, T. Baumbach, H. Suhonen, Comparison of image quality in computed laminography and tomography, *Optic Express* 20 (2012) 794-806.

- [5] Ahmad Mohamed Anwar, Mahmoud M. Osman, Dalia Elfiky, Gamal Hassan ,Performance Evaluation of Selected Irradiated Space Structure Composites Manufactured by the Hand Lay-Up Method, *International review of aerospace Ingineering*, *IREASE*, *Voll1*, *No04*, 2018
- [6] S. Gondrom, J. Zhou, M. Maisl, H. Reiter, M. Kröning, W. Arnold, X-ray computed laminography: an approach of computed tomography for applications with limited access, Nucl. Eng. Des. 190 (1999). [7] C Schorr and M Maisl, 'Exploitation of Geometric a Priori Knowledge for Limited Data Reconstruction in Non-Destructive Testing', Proceedings of the Fully Three-Dimensional Image Reconstruction in Radiology and Nuclear Medicine, Lake Tahoe, CA, 16, pp114-*117, (2013).*
- [8] Tamer Mekky Habib, Reham Abdellatif Abouhogail, Modelling of Spacecraft Orbit via Neural Networks, (International review of Aerospace engineering IREASE, Vol 14,No5,2021)
- [9] Ahmed Bacha, AA. Oukebdanne, AH. Belbachir, Virtual Improvement of Angular Resolution of a Tomographic Acquisition System, (International Journal on Engineering applications IREA Vol 2, No 3 (2014))
- [10] AHMED BACHA M.R OUKEBDANE.A BELBACHIR.A IMPLEMENTATION OF THE ZERO-PADDING INTERPOLATION TECHNIQUE TO IMPROVE ANGULAR RESOLUTION OF X-RAY TOMOGRAPHIC ACQUISITION SYSTEM ,(Pattern Recognition and Image Analysis 26(4):817-823)
- [11] S. Gondrom, J. Zhou, M. Maisl, H. Reiter, M. Kroning and W. Arnold, X-ray computed laminography: An approach "of computed tomography for applications with limited access, (Nucl Eng Des 190(1–2) (1999), 141–147).
- [12] L. Helfen, F. Xu, H. Suhonen, L. Urbanelli, P. Cloetens and T. Baumbach, Nanolaminography for three-dimensional high-resolution imaging of flat specimens, (*J Instrum* 8(5) (2013), C05006–C05006).
- [13] L. Helfen, T. Baumbach, P. Pernot, P.

- Mikul'ık, M. DiMichiel and J. Baruchel, Highresolution three-dimensional imaging by synchrotron-radiation computed laminography, (*Proc SPIE 6318 (2006), 63180N*).
- [14] L. Helfen, F. Xu, H. Suhonen, P. Cloetens and T. Baumbach, Laminographic imaging using synchrotron radiation, challenges and opportunities, (*J Phys Conf Ser 425(19) (2013)*, 192025)
- [15] Hatamikia, Sepideh, et al, "Optimization for customized trajectories in Cone Beam Computed Tomography,(*Med. Phys.*,(2020).doi:10.1002/mp.14403).
- [16] Ali Dinc, Mohammad B, Abdullah B, Ali A, Abdulaziz H, Faisal A, Nourah A, Mohamed A, Ahmed Mohamed A, A Performance-Based Parametric Design Exploration Tool for Student Aircraft Design Projects, (International review of Aerospace Engineering IREASE, VOL 16 No2 (2023)).
- [17] J. M. Ollinger, Maximum-likelihood reconstruction of transmission images in emission computed tomography via the EM algorithm, *IEEE Trans. Med. Imaging, vol. 13, no. 1, pp. 89-101, Mar. 1994, doi:* 10.1109/42.276147.
- [18] Zhao, Yunsong, et al. Edge information diffusion-based reconstruction for cone beam computed laminography, *IEEE Trans. Image Process.*, 27.9 (2018): 4663-4675. [19] D. O. Thompson, and D. E. Chimenti, "Review of progress in quantitative nondestructive evaluation, (Springer Science & Business Media, 2012)
- [20] B D Liu, J Bennett, G Wang, B De Man, K Zeng, Z Y Yin, et al., Completeness Map Evaluation Demonstrated with Candidate Next-Generation Cardiac CT Architectures, (Medical Physics, Vol 39, pp 2405-2416, 2012.)
 [21] G Wang, T Lin, P Cheng, and D Shinozaki, Cone-Beam Reconstruction of Plate-Like Specimens, (Journal of Scanning Microscopy, 1992, Vol 14, pp 350-354,).